Effects of AC-interference on chloride-induced corrosion of reinforced concrete

Andrea Brenna, Silvia Beretta, Fabio Bolzoni, MariaPia Pedeferri, Marco Ormellese *

Politecnico di Milano, Dipartimento di Chimica, Materiali e Ingegneria Chimica ''Giulio Natta'', Via Mancinelli, 7, 20131 Milano, Italy

HIGHLIGHTS

- AC interference weakens the passive layer of carbon steel in concrete.
- AC interference reduces the passive interval.
- Even at low current densities, AC decreases the $[Cl^-]/[OH^-]$ molar ratio.
- Corrosion rate in concrete is negligible if AC is lower than 30 A/m^2.

GRAPHICAL ABSTRACT
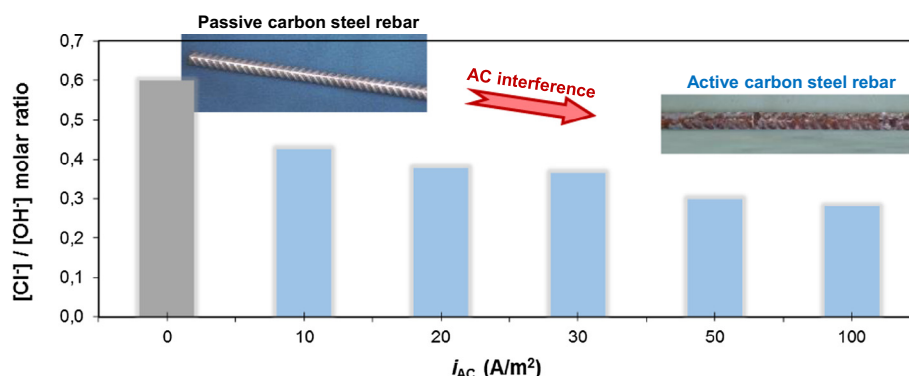
AC interference is a cause of reinforcement corrosion. Since few data are available, the influence of AC on the localized corrosion on passive carbon steel in concrete is discussed based on tests performed in alka-line solution and in concrete slabs. AC was applied in the range 10–500 A/m^2. Results allow stating that AC interference weakens steel passivity, increasing the passive current density, reducing both the passive interval and the $[Cl^-]/[OH^-]$ molar ratio. Results confirmed that the critical alternate current density is in the range 30–100 A/m^2, depending on the level of chlorides present into concrete.

1. Introduction

Carbon steel reinforcement in concrete are in passive condition due to alkalinity of the concrete pore solution, which promotes the formation of a thin passive layer. Rebar corrosion is due to a loss of the passive condition caused by concrete carbonation or chloride ingress [1]. In the latter case, corrosion occurs when the chloride content at the rebar level exceed a critical value. The threshold depends on several parameters [2–4]. Most important are: con-

crete pH (the concentration of hydroxyl ions in the pore solution), presence of voids at the interface rebar-to-concrete and electrochemical potential of the steel. Alkalinity mainly depends on cement type. Some authors [5,6] indicate a correlation between corrosion initiation and the chloride-to-hydroxyl ions molar ratio: corrosion does not occur when the ratio is lower than 0.6, corrosion is almost certain when the ratio exceed 1. A great variability of values is reported [2–4] as a direct consequence of the stocastic nature of initiation of chloride-induced corrosion on passive metals [7]; consequently, the chloride threshold is defined on a statistical basis. Macroscopic voids may strongly influence the chloride threshold [8]. Voids due to wrong concrete compaction may favour

* Corresponding author.
E-mail address: marco.ormellese@polimi.it (M. Ormellese).

Published Journal Article available at: http://dx.doi.org/10.1016/j.conbuildmat.2017.01.087

local acidification of the pore solution at the rebar-to-concrete interface, than reduction pH and the strength of the carbon steel passive layer, strongly reducing the critical chloride level. The electrochemical potential of carbon steel rebar, primarily related to the oxygen availability into concrete, plays the most important role in defining the critical chloride threshold. Higher is the oxygen content, higher is the electrochemical potential. For instance, decreasing carbon steel potential, chloride threshold can increase by one order of magnitude [9]. For reinforced concrete structure exposed to atmosphere, the typical free corrosion potential is in the passive range (+0.1/−0.2 V CSE). In this condition, the critical chloride ratio ranges from 0.4 % to 1.0% with respect the cement weight, confirming the wide range of the critical interval. Field data on a large number of structures [4,10] showed that the probability of corrosion is zero if the chloride content is lower than 0.2%, it increases to 20–30% at chloride content 0.4%, it reaches more than 70% if the chloride level is greater than 1%.

Stray currents flowing through the electrolyte concrete may influence the electrochemical potential of carbon steel rebars [1,11]. Consequently, the chloride-induced corrosion as well as the critical chloride threshold may be affected. Several types of concrete structures may suffer stray current induced corrosion: tunnels of the railway networks, bridges, foundations, and all the concrete structures parallel to railways or high voltage power lines. Reinforcements can pick up the stray current and anodic or cathodic interference may occur.

Stray current may be DC or AC depending upon the source. While for DC stray current induced corrosion on reinforced concrete structures there is large agreement on the criteria to be used for its mitigation and international standards are available since many years [12–14], in the presence of AC interference on reinforced concrete structures few data are available. AC-induced corrosion, instead, continues to be a controversial subject, and many aspects of it need to be clarified, especially the relationship between AC density and corrosion rate.

AC interference may occur if a reinforced concrete structure is parallel to an AC source, as in the case of reinforced concrete viaducts parallel to AC powered traction system or AC high-tension transmission lines [15]. In the last 10 years, at least in Italy, a new interference condition occurred because of the overlapping of high current AC traction systems (powered at 25 kV and 50 Hz), and the traditional direct current traction systems that have been operating for about a century.

Attention should also be dedicated to possible negative synergistic effects of AC and DC stray currents on the depassivation of passive carbon steel [1]. According to Bertolini et al. [1,15,16], the effects of AC current on passive carbon steel in concrete are more complex than the effects promoted by DC current, and typically the AC interference is much less dangerous than direct current.

AC interference is significant only on reinforced concrete structures, such as viaducts, which are parallel to the AC source: if the parallelism is in the order of hundreds of meters, AC current densities as high as some hundreds of A/m² [15,17] are expected.

In this context, the effect of AC interference on passive metals corrosion is a novelty, particularly regarding the influence of AC on electrochemical parameters such as the passive current density, the trans-passive potential and the passivity range. AC current may also affect the chloride threshold and may stimulate macro cells current that take place in the concrete between passive and corroding steel and can increase the corrosion rate on corroding steel in chloride-contaminated concrete.

From an electrochemical point of view, the behavior of passive carbon steel rebar in concrete (i.e. alkaline environment) is similar to the passive condition reached on cathodically protected carbon steel pipelines buried in soil [11]. In fact, during cathodic protec-tion, at the steel surface oxygen reduction occurs, which promotes oxygen consumption and hydroxyl ions production. pH at the steel surface can reach values close to 12–13. Since AC corrosion in soil has been studied since many years [17–23] and international standard are available [24], in order to define the AC interference effect on electrochemical parameters, a literature review regarding AC corrosion on buried pipeline has been performed.

Yunovich and Thompson [18] proposed an AC corrosion mechanism based on a conventional electrochemical approach. Because of the asymmetry of the anodic and cathodic potential-current density curves, such as in the case of passive carbon steel in concrete, under AC interference the shift of the corrosion potential differs from the current shift. The mean corrosion rate for a single AC imposed signal is greater than the corrosion rate in the absence of AC, i.e. a single AC cycle signal produces a net anodic current. This is the so-called faradaic rectification model.

Goidanich et al. [19] studied the effect of AC on overpotential of anodic and cathodic processes, specifically on Tafel slopes, exchanged current densities, equilibrium potentials and free corrosion potentials. On active metals, such as corroding rebar, the increase of corrosion rate is attributed to a decrease of the anodic and cathodic overpotentials and to an increase of exchange current densities of the two electrochemical processes. On passive metals, such as carbon steel rebar in alkaline concrete, AC weakens the passivity by reducing the anodic overpotential, promoting an increase of passive current density and a decrease of the transpassive potential. In the presence of chloride ions pitting potential shifts to more negative values [20].

Other authors [21,22] correlated the AC corrosion to the ratio of the anodic and cathodic Tafel slopes. If anodic and cathodic potential-current curves are asymmetric, as in the case of passive steel in aerated concrete, when an external sinusoidal voltage is applied, a shift of the corrosion potential is measured.

The European Technical Specification, EN 15280 [24] lists several parameters to evaluate AC corrosion likelihood: alternate voltage of an interfered structure, AC current density, resistivity and chemical composition. From on-field experience and laboratory tests, the primary parameters are alternate voltage and AC current density, the latter being the most accurate one. Following threshold are reported: maximum alternate voltage 15 V, maximum AC current density 100 A/m²; no corrosion risk if AC current density is lower than 30 A/m². Laboratory tests as well as field data [15,16,23] revealed possible AC corrosion even at very low AC current density (10 A/m²) on passive metals.

In order to study the influence of AC interference on the chloride-induced corrosion on passive carbon steel in concrete, to determine the effect of kinetics parameters and to estimate the possible chloride threshold reduction, corrosion tests has been performed in both alkaline solution and concrete slabs. AC current density was applied in the range of 10 A/m² up to 500 A/m²: values has been selected based both on specific literature review dealing with stray current in concrete [14–16] and the typical AC current density affecting the passive carbon steel pipeline in soil under cathodic protection condition [23,24]. In fact, considering reinforced concrete, AC current density lower than 30 A/m² is typical considered not dangerous, whereas AC corrosion is almost certain at 100 A/m², which is considered the maximum expected AC current density in concrete [14]. Nevertheless, to understand the AC mechanism and define the AC effect on the electrochemical parameters, tests have been performed also at very high values.

2. Materials and methods

The influence of AC interference on the passivity of carbon steel in concrete was firstly studied by means of anodic potentiody-

namic curves (E-log *i* curves) to identify AC influence on passivity range, transpassive potential and passive current density. Immersion tests (50 day long) and tests in concrete (1 year long) were performed to evaluate the effect of AC on the critical chloride threshold for corrosion initiation.

2.1. Potentiodynamic tests

Carbon steel specimens (10 mm in diameter, 20 mm long) were cut from commercial reinforcing steel, degreased in acetone then sandblasted. The net exposed surface area was 80 mm^2.

Tests were performed in a four-electrode cell: the carbon steel specimen, a saturated calomel reference electrode (SCE, +0.244 V SHE), a platinum counter-electrode to supply the DC current and a Ti-MMO (Mixed Metal Oxides) counter electrode to overlap the AC interference.

Due to the simultaneous presence of an AC and a DC signal, a dedicated electric circuit was used, to supply and measure AC and DC signals independently. The circuit consists of two different meshes (Fig. 1). Within AC mesh, AC from a feeding system (variac, frequency 50 Hz) flows between the specimen (working electrode, W) and an activated titanium counter electrode (CE$_{AC}$) through a 10 Ω, 250 W shunt, R1; two electrolytic 1000 μF capacitors in series (total capacity of 500 μF and a capacitive reactance of about 6 Ω) prevent DC circulation. Within DC mesh, DC current is supplied by a galvanostat/potentiostat and it flows between the specimen (working electrode, W) and a second activated titanium counter electrode (CE$_{DC}$) through a 10 Ω, 10 W shunt, R2; a 20 H inductor reduces AC circulation to less than 1%. The inductive reactance of a 20 H inductor is about 6300 Ω. AC and DC meshes share a common branch, where AC and DC overlap and flow to the working electrode (W) through a variable shunt, R3, whose value is selected under experimental conditions (from 1 Ω up to 100 Ω). The circuit was tested under different conditions. It was confirmed that the efficiency of the DC filter was 100%, i.e., no DC flowed in the AC mesh. Instead, despite a 20 H inductance, a small part of the AC, less than 1% of the total AC, flowed in the DC mesh, negligible for the planned tests.

Anodic potentiodynamic tests were performed with an EG&G Princeton Applied Research potentiostat/galvanostat, starting from the open circuit potential up to +1.2 V SCE, with a potential scan rate of 0.2 mV·s^{-1}. Specimens were immersed in a synthetic alkaline concrete pore solution [1]: saturated calcium hydroxide with NaOH 0.01 mol/L (pH = 12.6). No pH variations were measured before and after each test. Tests were performed under temperature control (20 °C ± 1 °C) by means of a thermostatic bath, placing a thermometer in the cell. Seven levels of AC current density were applied with an AC feeder (frequency 50 Hz, internal impedance 10 MΩ), according to the threshold reported in literature [5,17–18]: 10, 30, 50, 100, 300 and 500 A/m^2. Highest values were tested to simulate very severe interfering conditions. Feeding alternate voltage ranged from 2 V up to 10 V. For comparison purposes, tests in the absence of any AC interference were performed. For each condition, tests were performed in duplicate.

2.2. Immersion tests

Carbon steel specimens (10 mm in diameter, 40 mm long) were cut from commercial reinforcing steel, degreased in acetone then sandblasted. Specimens were immersed in a polymeric cylindrical cells (diameter 19 cm, height 15 cm) filled with 3 L of the same synthetic alkaline concrete pore solution used in the previous tests. Tests were performed under temperature control (20 °C ± 1 °C) by means of a thermostatic bath, placing a thermometer in the cell. AC was applied by means of a variac (frequency 50 Hz, internal impedance 10 MΩ). Eight values of AC current density were applied: 10, 20, 30, 40, 50, 100, 300 and 500 A/m^2. Highest values were tested to simulate very severe interfering conditions. Feeding alternate voltage ranged from 2 V up to 10 V. For each AC current density, two test cells were assembled, each containing two carbon steel specimens. In the first week, solution was chloride-free to allow a stable passive layer formation on carbon steel; then AC was overlapped and 0.002 mol/L of chlorides were added every 48 h for 50 days. Control tests were performed on freely corroding carbon steel specimens, in the absence of any AC interference. Corrosion was constantly monitored by carbon steel potential measurements and by visual inspection.

2.3. Concrete tests

Concrete slabs (120 × 120 × 50 mm) were cast with Ordinary Portland Cement (CEM I 42.5R according to EN 197 [25]), W/C ratio 0.6 and a 1770 kg/m^3 of crashed limestone aggregates (20 mm maximum diameter). Five classes of aggregates were used, following the Fuller distribution. An acrylic-based superplasticizer (0.6% by cement weight) was added to the concrete mixture to assure high workability (slump in the range of 150–210 mm). Table 1 resumes the used mixture proportion. Slabs were cured 28 days at 95% RH. Mean compressive strength, measured on three cubic specimens after 28 days curing, was 39.9 MPa.

Two carbon steel rebars (10 mm in diameter and 130 mm length) were placed in each concrete slab (Fig. 2). In order to apply high AC current density values (higher than 100 A/m^2), rebars were
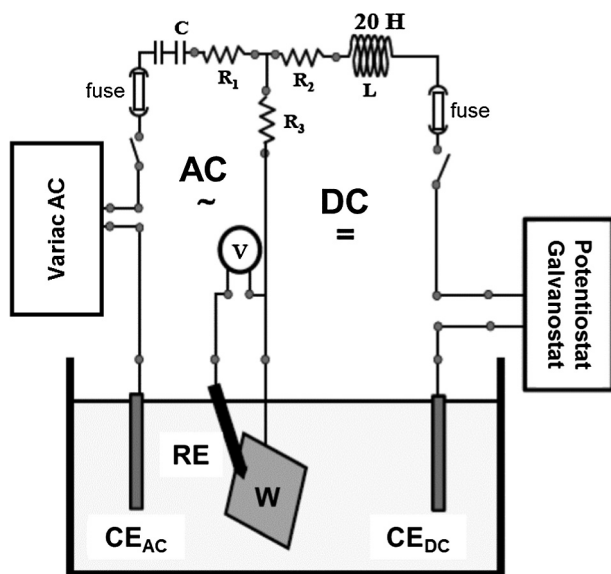

Fig. 1. Electric circuit with DC and AC separation.

Table 1
Concrete mixture proportion.

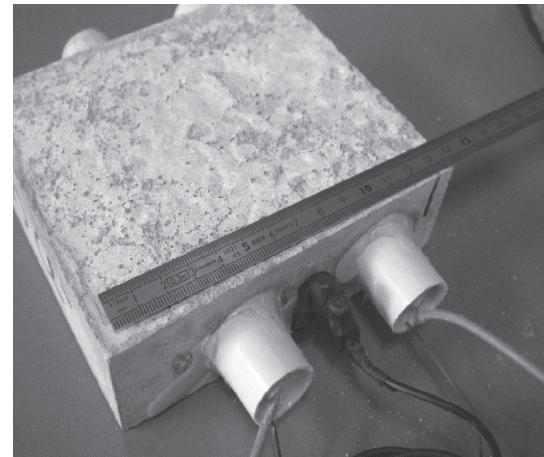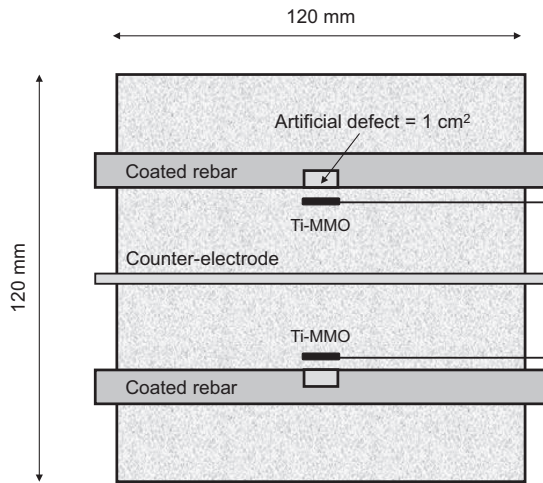|	Type	Dosage	
W/C ratio		0.6	
Cement	CEM I 52,5 R	367 kg/m^3	
Water	Fresh water	220 L/m^3	
Aggregates	Gravel 10–20 mm	35%	620 kg/m^3
	Gravel 8–10 mm	15%	265 kg/m^3
	Gravel 0–8 mm	15%	265 kg/m^3
	Sand 0.25 mm	15%	265 kg/m^3
	Limestone 0.075 mm	20%	355 kg/m^3
	Total	100%	1770 kg/m^3
Superplasticizer	Acrylic-based	0.60% cement weight	
Chlorides	NaCl	0.25% cement weight	

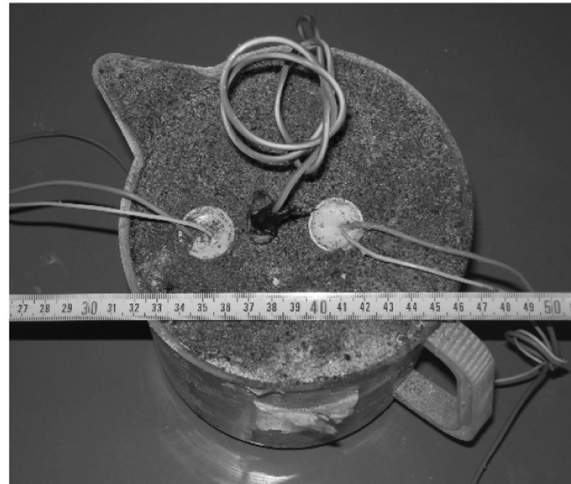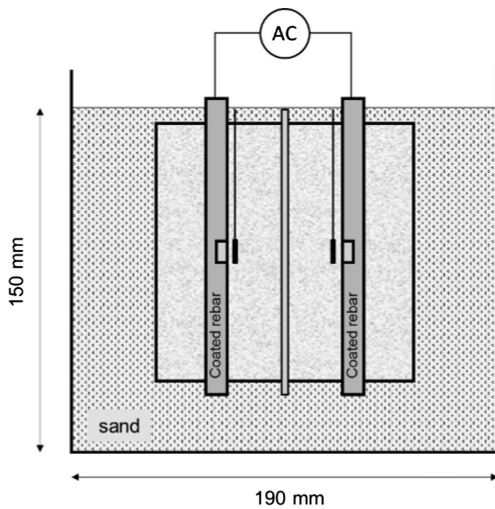**Fig. 2.** Concrete slab.

Fig. 3. Concrete slab in the cylindrical cell.

sand-blasted, painted with an epoxy resin-based coating, and a defect 100 mm^2 wide was created at the centre of each rebar. In fact, on real structures, since steel reinforcements are usually uncoated, the interference current spreads along a large exposed surface, which may lead to much smaller current densities.

Concrete cover was 20 mm thick.

To simulate concrete foundation, each concrete slab was placed in a cylindrical cell (diameter 19 cm, height 15 cm, Fig. 3) filled with water saturated soil-simulating sand (1200 mg/L of SO_4^{2-}; 200 mg/L of Cl^-; electrical resistivity 40 Ω·m). Temperature was controlled once a week by placing a thermometer in the sand: mean value was 20 °C (±3 °C).

Three levels of AC current density were applied between the two rebars in each concrete specimen, by means of an AC variac (frequency 50 Hz, internal impedance 10 MΩ): 10, 100 and 500 A/m^2. The highest value, not typical for real reinforced concrete structures, was tested to understand the AC mechanism. Feeding alternate voltage ranged from 5 V up to 15 V.

AC interference was continuously applied, simulating the worst scenario, promoted by AC high-tension transmission lines. On real reinforced concrete structures, AC interference can be discontinuous if the source is an AC powered traction system. In the latter case, AC effect may be mitigated both by depolarization of steel and diffusion phenomena through the concrete pores in the periods of absence of AC current.

For each interfering condition, four concrete specimens were cast: two without added chlorides and two with a chloride content of 0.25% by cement weight (value lower than the minimum of the critical chloride interval, which is typically considered in the range 0.4–1% with respect cement weight [1]). For comparison purposes, tests in absence of AC interference were also performed.

Tests last 1 year, during which corrosion was monitored by measuring the rebar potential with respect to an internal Ti-MMO reference electrode (−0.05 V SCE) placed close to the artificial defect, and by corrosion rate evaluation. In the results section, potential readings are plotted with respect an SCE reference electrode. Corrosion rate was determined by means of linear polarization resistance technique (LPR), applying a potential scan rate of 10 mV/min in the range ±10 mV with respect to the free corrosion potential. During the reading, AC signal was switched off. Mean corrosion rate, C_{rate} (in μm/y) was evaluated applying the Stern-Geary equation [26]:

$$C_{rate} = 1.17 \cdot B/LPR \qquad (1)$$

where *B* is equal to 52 mV for passive carbon steel and 26 mV for active one, and *LRP* (in $\Omega \cdot m^2$) is the measured linear polarization resistance. *LRP* is typically used to measure on-line corrosion rate on active metals. Nevertheless, Andrade et al. [27–29] demonstrated a good correlation between LRP measurements and effective mass loss even in the case of localized corrosion of carbon steel in concrete. At the end of the test, carbon steel rebars were extracted from concrete specimens and they were subjected to visual inspection.

3. Results

3.1. Potentiodynamic tests

Fig. 4 shows anodic potentiodynamic curves of carbon steel in alkaline solution in the presence of AC interference. The initial free corrosion potential is in the range 0 mV/−200 mV SCE, regardless the AC interference. In the absence of AC, the typical carbon steel passive curve was obtained: passive interval is 950 mV wide, starting from −100 mV SCE up to 850 mV SCE (being the latter the transpassive potential); passive current density is close to 4 mA/m².

At 10 A/m² AC current density, free corrosion potential remained practically constant, while the transpassive potential reduces to +570 mV SCE. A small increase in passive current density was measured (6 mA/m²). At 30 A/m² AC current density, a further reduction of the transpassive potential was detected, while the passive current density remained almost constant, equal to the value measured in the presence of 10 A/m². In the presence of 50 and 100 A/m² AC current density, the anodic curves do not show any passive interval: carbon steel is completely in active condition. Anodic curves obtained at 300 A/m² and 500 A/m² AC current densities (not reported in Fig. 4) are overlapped to the curve obtained at 100 A/m².

3.2. Immersion test

Fig. 5 reports potential monitoring of carbon steel specimens immersed in alkaline solution: only five AC current density levels (10, 20, 30, 40 and 50 A/m²) are plotted; at higher AC values results are similar to the one obtained at 50 A/m². For each current density, only one carbon steel sample is plotted. Every 2 days, 0.002 mol/L of chlorides were added into the solution.

Before any chloride addition, free corrosion potential of all the carbon steel specimens was in the range −100 mV and −250 mV
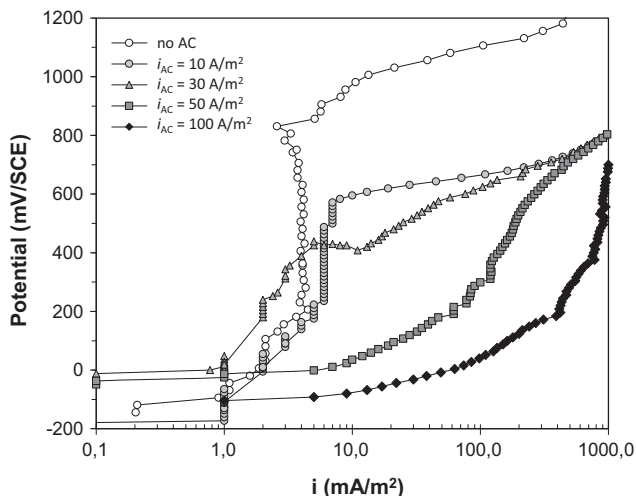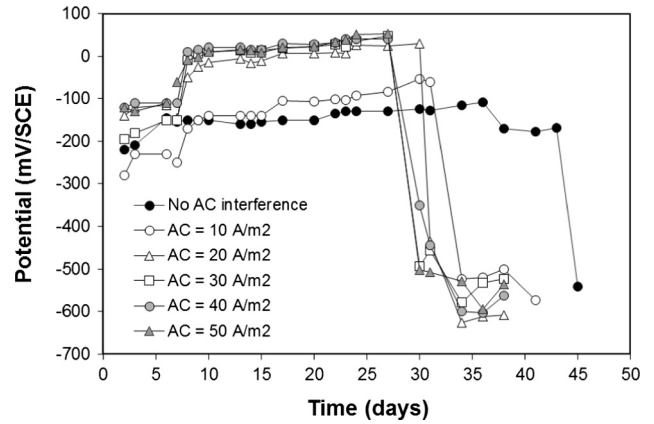

Fig. 5. Free corrosion potential of carbon steel in synthetic alkaline concrete pore solution (pH 12.6) varying AC current density.

Table 2
Chloride content at the corrosion initiation of carbon steel in synthetic alkaline concrete pore solution.

AC (A/m²)	Chloride content at the corrosion initiation (mol/L)			
	Sample 1	Sample 2	Sample 3	Sample 4
0	0.028	0.028	–	–
10	0.016	0.016	0.018	0.018
20	0.014	0.014	0.016	0.016
30	0.012	0.014	0.016	0.016
40	0.012	0.012	0.012	0.012
50	0.012	0.012	0.014	0.014

SCE. In the absence of AC interference, corrosion potential decreases to −500 mV SCE, after 45 days of testing: the chloride content was 0.028 mol/L (Table 2). Corrosion products appeared on the carbon steel surface.

In the presence of 10 A/m² AC current density, free corrosion potential in passive condition remained stable, close to −200 mV SCE. At higher AC current density, potentials moved toward more positive values: higher the AC current density, higher the potential shift. After about 30 to 35 days of AC interference, corrosion potentials of all the carbon steel specimens decreased to −500 mV/−600 mV SCE. Chlorides content was in the range 0.012–0.018 mol/L. Presence of corrosion product on carbon steel specimens confirmed the initiation of corrosion.

Table 2 shows the chloride content once the corrosion was visually observed on the carbon steel specimen.

3.3. Concrete tests

Fig. 6 shows free corrosion potential profile and corrosion rate measurements performed on chloride-free reinforced concrete slabs in the presence of different of AC interference level.

In the absence of AC interference, corrosion potentials was in the range 0 mV to −150 mV SCE and corrosion rate was lower than 2 μm/y, i.e. reinforcements are in passive conditions and corrosion rate is negligible [1,27–29].

AC current density of 10 A/m² did not change corrosion condition: free corrosion potential was stable. Nevertheless, a slight increase in mean corrosion rate was measured. At 100 A/m² AC current density, more negative free corrosion potentials were measured: after about 250 days two rebars showed a free corrosion potential close to −300 mV SCE, and one of them an high corrosion rate. At 500 A/m² AC current density, more negative corrosion potentials were measured. Corrosion rate was not negligible, close to 100 μm/y.

Fig. 4. Potentiodynamic curves of carbon steel in synthetic alkaline concrete pore solution at different AC current density level.
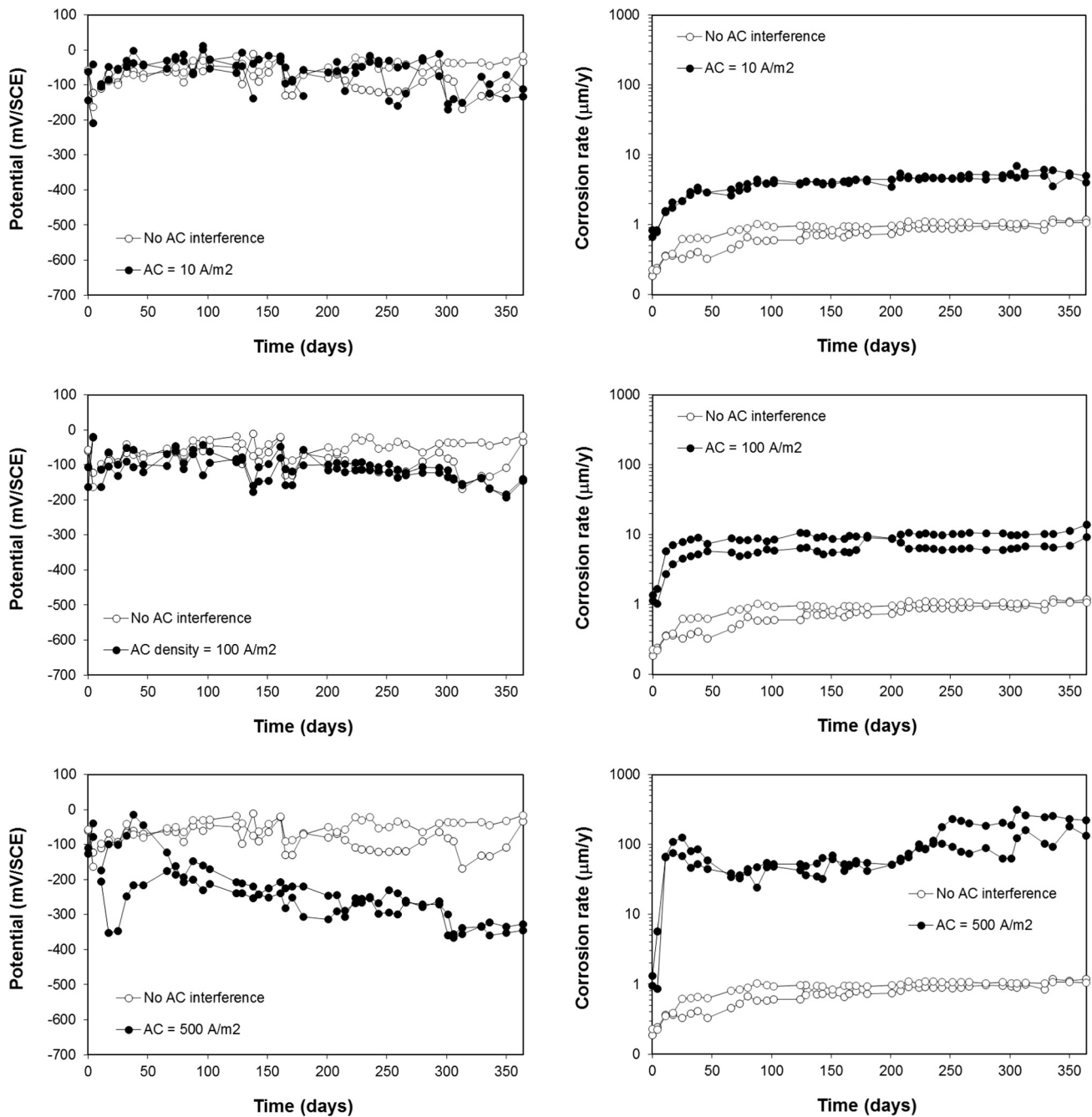
Fig. 6. Free corrosion potential and corrosion rate of rebar in concrete chloride-free varying AC current density.

Fig. 7 shows free corrosion potential profile and corrosion rate measurements of carbon steel rebars in concrete slabs in the presence of 0.25% chlorides by cement weight. In the absence of AC interference, corrosion potentials are in the range −100 mV/−200 mV SCE, and corrosion rate is lower than 2 μm/y, i.e. reinforcements are in passive conditions.

At AC current density 10 A/m², free corrosion potential remained almost stable; after about 250 days one rebar showed a potential decrease to −400 mV SCE. Rebars corrosion rate was in the range 5–30 μm/y, about one order of magnitude higher than in the absence of AC interference. At 100 A/m² AC current density, potentials shifted to more negative values. Corrosion rate was in the range 10–100 μm/y. At 500 A/m² AC current density, after

100 days of test, corrosion potential strongly decreased to −400/−500 mV SCE. Corrosion rate was higher than 100 μm/y.

After one-year test, carbon steel reinforcements were extracted from concrete specimens and visually inspected. At AC current density lower than 10 A/m² no corrosion was detected on the rebars. At 100 A/m² AC current density, corrosion occurred both in the absence and the presence of chlorides. Corrosion products have caused the partial detachment of the epoxy coating. At 500 A/m² AC current density, corrosion appeared uniformly on the whole rebar surface, even in the absence of chlorides.

Phenolphthalein test was performed on the surface of reinforced concrete slabs after breaking. At 500 A/m² AC current density, an acidification (pH < 10) of the first 3 mm of the cement
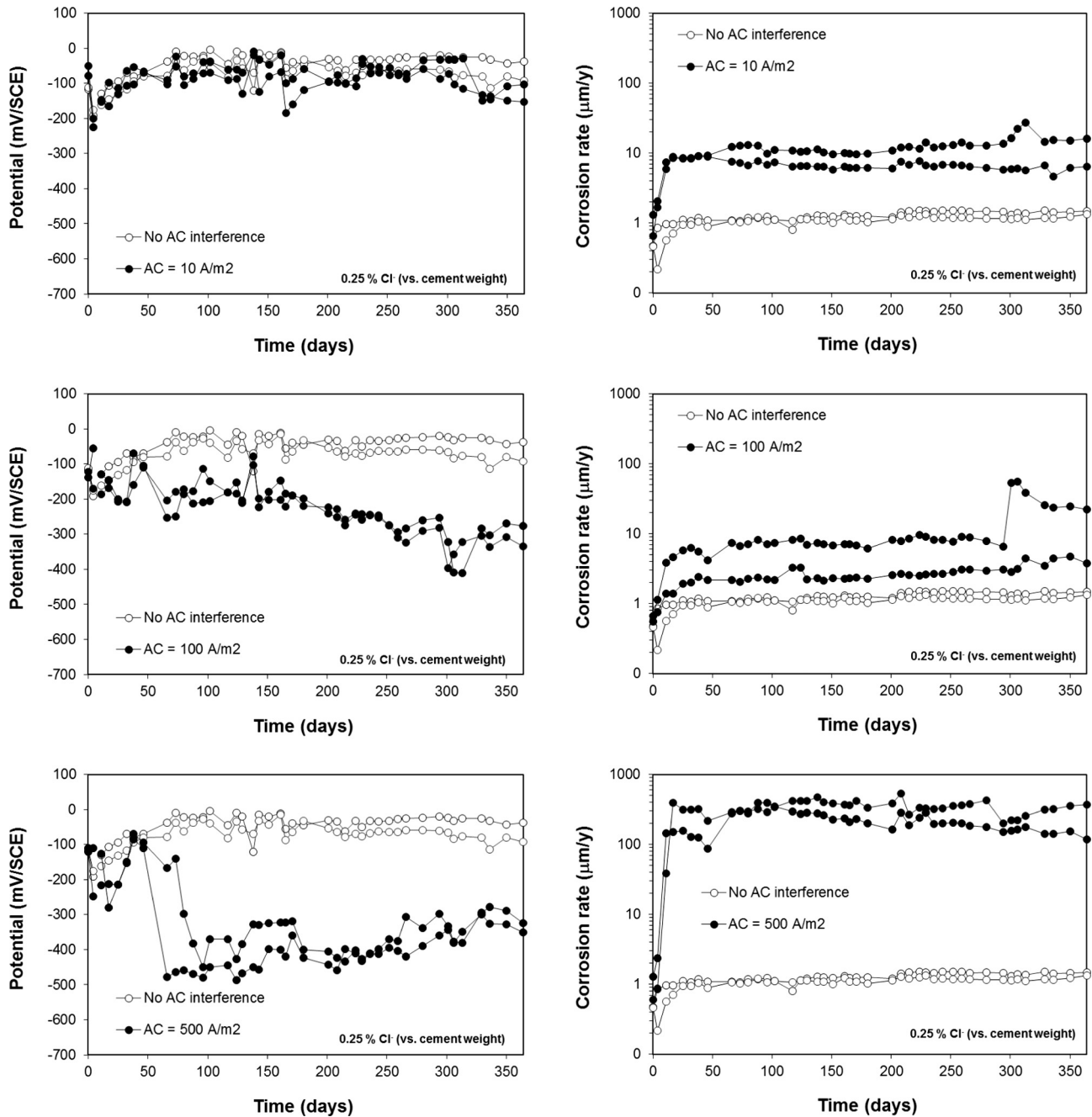
Fig. 7. Free corrosion potential and corrosion rate of rebar in concrete with chlorides (0.25% by cement weight) varying AC current density.

paste at the interface rebar-to-concrete was observed, both in the presence and absence of added chlorides.
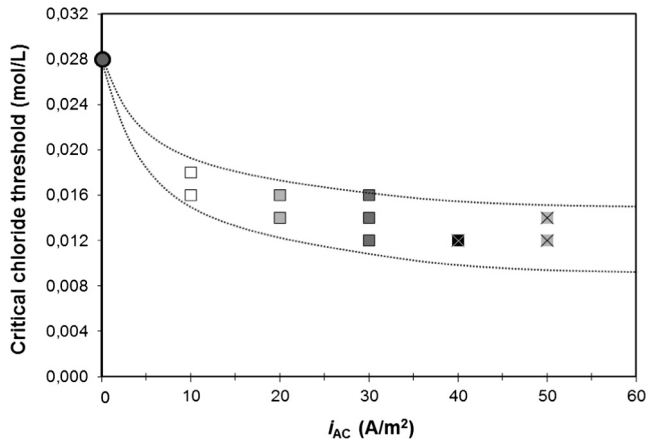
4. Discussion

In aerated chloride-free alkaline solutions (pH > 11.5) a protective oxide film, few nanometres thick, covers carbon steel. In these conditions, carbon steel is passive and its corrosion rate is practically negligible. The same happens in a properly cured and cast concrete, since the solution in the concrete pores has a pH in the range 13–13.5 [1]. Laboratory tests allow evaluating the effect of AC stray current on carbon steel passivity and the effect of such interference on the critical chloride threshold for corrosion initiation, and then on the service life of a reinforced concrete structure

exposed to a chloride-containing environment. AC current density was applied in the range of 10 A/m^2 up to 500 A/m^2, according to specific literature review dealing with stray current in concrete [14–16]. AC current density lower than 30 A/m^2 is typical considered not dangerous; AC corrosion is almost certain at 100 A/m^2, which is considered the maximum expected AC current density in concrete [14]. However, to evaluate the AC effect on corrosion of passive carbon steel, tests have been performed also at very high values. To reach such a high current densities, tests has been performed on small carbon steel samples and on coated carbon steel rebars. On real structures, steel reinforcements are usually not coated and the interference current may spread along a large exposed surface, which may lead to much smaller current densities. AC interference was continuously applied to simulate the worst scenario promoted by AC high-tension transmission lines.

Table 3

Free corrosion potential, transpassive potential, passive range and passive current density of carbon steel in synthetic alkaline concrete pore solution.

AC A/m^2	Free corrosion potential mV SCE	Transpassive potential mV SCE	Passive range mV	Passive current density mA/m^2
0	−119	831	950	4
10	−173	571	744	6
30	−12	439	451	6
50	−37	–	–	–
100	−94	–	–	–

Fig. 8. Critical chloride threshold in the presence of AC interference for carbon steel in synthetic alkaline concrete pore solution (pH 12.6).

Table 4

Free corrosion potential and corrosion rate of rebar embedded in concrete under AC interference.

AC A/m^2	No added chloride		Chloride 0.25% by cement weight	
	Free corrosion potential mV SCE	Corrosion rate μm/y	Free corrosion potential mV SCE	Corrosion rate μm/y
0	0/−150	<2	0/−200	<2
10	0/−150	<10	−100/−300	<30
100	−100/−300	10–30	−200/-500	<100
500	−200/−400	100	−300/−500	>100

4.1. AC effect of carbon steel passivity

Anodic polarization tests were carried out on carbon steel in aerated synthetic alkaline concrete pore solution to study the effect of AC interference on electrochemical parameters obtained in a potential-current curve, namely the passivity range and the passive current density, which are related to corrosion resistance of a passive metal. Table 3 summarises the obtained values.

AC interference does not affect free corrosion potential, whereas transpassive potential decreases as soon as AC current density increases. Consequently, the passive range reduces from 950 mV in the absence of AC, to 744 mV and 451 mV in the presence of 10 A/m^2 and 30 A/m^{2}AC current density, respectively. Accordingly, the passive current density increases. At AC current density higher than 50 A/m^2, passivity is completely destroyed. Tests clearly demonstrates that AC interference has a strong negative effect on the stability of the passive layer of carbon steel in alkaline condition. A similar effect was observed in previous experimental tests on cathodically protected carbon steel specimens in the presence

of AC interference [30–31]. In fact, from an electrochemical point of view, under cathodic protection condition carbon steel works in contact with a high alkaline solution that promotes carbon steel passivation, according to iron Pourbaix Diagram [32].

The presence of AC stray current weakens the passive layer promoting localized corrosion.

4.2. AC effect of critical chloride threshold

The second series of tests, performed in aerated synthetic alkaline concrete pore solution at increasing chloride concentration, allow evaluating the effect of AC interference on the critical chloride threshold to initiate corrosion.

In the absence of any interference, localized corrosion occurs on passive rebar once a critical chloride concentration is exceeded at the rebar level. The internationally accepted critical [Cl$^-$]/[OH$^-$] molar ratio is 0.6, corresponding to a critical chloride interval 0.4–1% with respect the cement weight for a reinforced concrete structures exposed to the atmosphere [1]. In a solution pH 12.6, taking into account the above-mentioned molar ratio, the critical chloride content is equal to 0.024 mol/L.

Fig. 8 resumes the chloride contents at which corrosion on carbon steel specimens was observed. In the absence of AC, the chloride content is 0.028 mol/L, in agreement with the critical [Cl$^-$]/[OH$^-$] molar ratio. In the presence of AC interference, the chloride content decreases to 0.018 mol/L in the presence of 10 A/m^2 AC current density, up to halved (0.014 mol/L) in the presence of an interfering AC current density higher than 30 A/m^2. It means that in the presence of AC interference the [Cl$^-$]/[OH$^-$] molar ratio is reduced to 0.30–0.45.

The weakening of the protective properties of the passive film on carbon steel results in a severe reduction of the critical chloride content for corrosion initiation. This effect was confirmed by concrete tests. Table 4 shows free corrosion potential and average corrosion rate of rebars in concrete under AC interference.

In the absence of chlorides, rebar are in passive condition, even in the presence of 10 A/m^2 AC current density: corrosion rate is negligible and free corrosion potential is in the typical range of passivity. Corrosion occurred at AC current density 100 A/m^2: free corrosion potential decreases and not acceptable values of corrosion rate were measured. At higher AC current density (500 A/m^2) corrosion rate is close to 100 μm/y. In the presence of chlorides, corrosion occurred even at the minimum level of AC interference (10 A/m^2). Higher is the AC level, higher is the rebar corrosion rate.

4.3. Effect of the concrete acidification

At high AC level, the pH of cement paste at the rebar-to-concrete interface is less alkaline, as demonstrated by phenolphthalein tests. Combining the effect of the [Cl$^-$]/[OH$^-$] molar ratio decrease and pH reduction, AC strongly reduces the critical chloride content for corrosion initiation. For examples, assuming a pH reduction to 10 and a [Cl$^-$]/[OH$^-$] molar ratio of 0.4, in the presence of AC interference the critical chloride content reduces from 0.024 mol/L (valid for alkaline concrete in the absence of AC) to 0.0004 mol/L.

5. Conclusions

The effect of AC-induced interference on the corrosion resistance of passive carbon steel was investigated throughout corrosion tests in aerated synthetic alkaline concrete pore solution as well as in concrete, both in the absence an in the presence of chlorides.

Tests performed in alkaline solution confirmed that AC interference weakens carbon steel passivity, reducing the passive interval and increasing the passive current density. In the presence of AC, the critical $[Cl^-]/[OH^-]$ molar ratio is reduced to 0.30/0.45.

Tests performed in reinforced concrete slabs showed that in the absence of chloride corrosion rate is negligible if AC current density is lower than 100 A/m^2; in the presence of chlorides, corrosion rate I negligible if AC current density is lower than 30 A/m^2.

References

[1] L. Bertolini, B. Elsener, P. Pedeferri, E. Redaelli, R.B. Polder, Corrosion of Steel in Concrete: Prevention, Diagnosis, Repair, second ed., John Wiley Sons, 2013.

[2] G.K. Glass, N.R. Buenfeld, Chloride threshold level for corrosion of steel in concrete, Corros. Sci. (1997) 1001–1013.

[3] U. Angst, B. Elsener, C.K. Larsen, O. Vennesland, Critical chloride content in reinforced concrete – a review, Cem. Concr. Res. 29 (2009) 1122–1138.

[4] M.C. Alonso, M. Sanchez, Analysis of the variability of chloride threshold values in literature, Mater. Corros. 60 (2009) 631–637.

[5] C.L. Page, P. Lambert, P.R.W. Vassie, Investigation of reinforcement corrosion: 1. The pore electrolyte phase in chloride-contaminated concrete, Mater. Corros. 24 (1991) 243–252.

[6] P. Lambert, C.L. Page, P.R.W. Vassie, Investigation of reinforcement corrosion: 2. Electrochemical monitoring of steel in chloride-contaminated concrete, Mater. Corros. 24 (1991) 351–358.

[7] T. Shibata, Corrosion probability and statistical evaluation of corrosion data, in: R.W. Revie (Ed.), Uhlig's Corrosion Handbook, John Wiley & Sons, New York, NY, 2000, pp. 367–390.

[8] G.K. Glass, N.R. Buenfeld, The inhibitive effects of electrochemical treatment applied to steel in concrete, Corros. Sci. 42 (2000) 923–927.

[9] L. Bertolini, F. Bolzoni, M. Gastaldi, T. Pastore, P. Pedeferri, E. Redaelli, Effect of cathodic prevention on the chloride threshold for steel corrosion in concrete, Electrochim. Acta 24 (2009) 1452–1463.

[10] R.B. Polder, Critical chloride for reinforced concrete and its relationship to concrete resistivity, Mater. Corros. 60 (2009) 623–630.

[11] L. Lazzari, P. Pedeferri, Cathodic Protection, first ed., Polipress Milan, Italy, 2006.

[12] EN 50162, Protection Against Corrosion by Stray Current From Direct Current Systems, 2005.

[13] EN 1992-1-1 (Eurocode 2), Design of Concrete Structures, 2004.

[14] NACE 01110, Stray Current Induced Corrosion in Reinforced and Pre-Stressed Structures, Item No. 24241, NACE – NACE International, Houston, TX, 2010.

[15] NACE 35110, AC Corrosion State-of-the-Art: Corrosion Rate, Mechanism, and Mitigation Requirements, Item No. 24242, NACE – NACE International, Houston, TX, 2010.

[16] L. Bertolini, M. Carsana, P. Pedeferri, Corrosion behaviour of steel in concrete in the presence of stray current, Corros. Sci. 49 (3) (2007) 1056–1068.

[17] EN 50443, Effects of Electromagnetic Interference on Pipelines Caused by High Voltage AC Electric Traction Systems and/or High Voltage AC Power Supply Systems, 2011.

[18] M. Yunovich, N.G. Thompson, AC corrosion: mechanism and proposed model, in: Proceedings of IPC (International Pipeline Conference), Paper No. 0574, ASME (American Society of Mechanical Engineers) International, Calgary (CDN), 2004, pp. 183–195.

[19] S. Goidanich, M. Ormellese, L. Lazzari, Effect of AC interference on cathodic protection monitoring, Corros. Eng. Sci. Technol. 46 (2011) 618–623.

[20] M. Ormellese, L. Lazzari, A. Brenna, Effects of AC-interference on passive metals corrosion, in: Proc. Int. Conf. Corrosion/2011, Paper No. 11342, NACE, Houston, TX, 2011.

[21] S.B. Lalvani, X. Lin, A revised model for predicting corrosion of materials induced by alternating voltages, Corros. Sci. 38 (10) (1996) 1709.

[22] U. Bertocci, AC induced corrosion. the effect of an alternating voltage on electrodes under charge-transfer control, Corrosion 35 (5) (1979) 211.

[23] P. Linhardt, G. Ball, AC Corrosion: Results from Laboratory Investigations and from a Failure Analysis, CORROSION/2006, Paper No. 06160, NACE, Houston, TX, 2006.

[24] EN 15280, Evaluation of AC Corrosion Likelihood of Buried Pipelines – Application to Cathodically Protected Pipelines, 2013.

[25] EN 197/1, Cement: Part 1. Composition, Specifications and Conformity Criteria for Common Cements, 2000.

[26] J.A. Gonzalez, A. Molina, M.L. Escudero, C. Andrade, Errors in the electrochemical evaluation of very small corrosion rates: I. Polarization resistance method applied to corrosion of steel in concrete, Corros. Sci. 25 (1985) 917.

[27] C. Andrade, J.A. Gonzalez, Quantitative measurements of corrosion rate of reinforcing steels embedded in concrete using polarization resistance measurements, Werkst. Korros. 29 (1978) 519.

[28] C. Andrade, M.C. Alonso, J.A. Gonzalez, An initial effort to use the corrosion rate measurements for estimating rebar durability, in: Symposium on Corrosion rate in Reinforcement in Concrete, ASTM, Baltimore, 1988.

[29] G. Baronio, M. Berra, L. Bertolini, T. Pastore, Steel corrosion monitoring in normal and total-lightweight concretes exposed to chloride and sulphate solutions part II: Polarisation resistance measurements, Cem. Concr. Res. 26 (1996) 691–696.

[30] A. Brenna, M.V. Diamanti, L. Lazzari, M. Ormellese, A proposal of AC corrosion mechanism in cathodic protection, Technical Proc. of the 2011 NSTI Nanotechnology Conf. and Expo, NANOTECH 2011, TechConnect World – Conf. & Expo, vol. 3, CRC Press – Taylor & Francis Group, Boston, MA, 2011. ISBN 978-1-4398-7138-6.

[31] A. Brenna, M. Ormellese, L. Lazzari, Electromechanical breakdown mechanism of passive film in alternating current-related corrosion of carbon steel under cathodic protection condition, Corrosion 72 (8) (2016) 1055–1063.

[32] M. Pourbaix, Atlas of Electrochemical Equilibria in Aqueous Solutions, second English ed., NACE, Houston, TX, 1974.